ORIGINAL PAPER

Extreme tadpoles II: the highly derived larval anatomy of *Occidozyga baluensis* (Boulenger, 1896), an obligate carnivorous tadpole

Alexander Haas · Jana Pohlmeyer ·
David S. McLeod · Thomas Kleinteich ·
Stefan T. Hertwig · Indraneil Das · Daniel R. Buchholz

Abstract Tadpoles of *Occidozyga* species have been reported to be carnivorous, feeding on insects and other tadpoles. We present photographic evidence for the previously undocumented larval feeding behavior in *O. baluensis*. Furthermore, we present a detailed anatomical description of the skull, cranial musculature, and gross gut morphology based on three-dimensional reconstructions from serial sections and µCT imagery. The cranial anatomy of larval *O. baluensis* is highly derived in many characters, with respect to taxa outside the genus *Occidozyga*, most notably the palatoquadrate and hyobranchial apparatus, that play a major role in tadpole feeding. A large larval stomach was present in the specimens examined, indicative of a macrophagous carnivorous mode of feeding. Because of the relatively small oral orifice, relatively large-sized food items found in the larval stomach, and the tunnel-like arrangement of structures that form the buccal cavity, we hypothesize that suction feeding utilizing strong negative pressure is employed by this species. Furthermore, we propose that force, rather than speed, is the main characteristic of their feeding. The unique features of the study species substantially expand the known morphospace for tadpoles, particularly among the Acosmanura (Pelobatoidea, Pelodytoidea, and Neobatrachia). Except for Microhylidae, acosmanurans previously described possess limited innovative larval morphologies. Larval carnivory has evolved convergently several times in distant anuran clades and shows structural, behavioral, and functional differences in the known examples.

Keywords Lissamphibia · Anura · Dicroglossidae · Carnivory · Cranium · Larval stomach

A. Haas (✉) · J. Pohlmeyer
Biozentrum Grindel und Zoologisches Museum Hamburg,
Martin-Luther-King-Platz 3, 20146 Hamburg,
Germany
e-mail: alexander.haas@uni-hamburg.de

J. Pohlmeyer
e-mail: janapohlmeyer@hotmail.de

D. S. McLeod
University of Kansas Biodiversity Institute, 1345 Jayhawk
Boulevard, Lawrence, KS 66045-7561, USA
e-mail: dsmcleod@ku.edu

T. Kleinteich
Functional Morphology and Biomechanics, Christian-Albrechts-
Universität Kiel, Am Botanischen Garten 1–9, 24098 Kiel,
Germany
e-mail: tkleinteich@zoologie.uni-kiel.de

S. T. Hertwig
Naturhistorisches Museum der Burgergemeinde Bern,
Bernastrasse 15, 3005 Bern, Switzerland
e-mail: stefan.hertwig@nmbe.ch

I. Das
Institute of Biodiversity and Environmental Conservation,
Universiti Malaysia Sarawak, 94300 Kota Samarahan, Sarawak,
Malaysia
e-mail: idas@ibec.unimas.my

D. R. Buchholz
Department of Biological Sciences, University of Cincinnati,
711A Rieveschl Hall, 312 Clifton Ct., Cincinnati, OH 45221,
USA
e-mail: buchhodr@ucmail.uc.edu

Abbreviations

3D	Three-dimensional
cart.	Cartilago
for.	Foramen
lev.	Levator
m.	Musculus
mand.	Mandibulae
proc.	Processus
prof.	Profundus

Introduction

Most anuran amphibian species have complex life cycles, where distinct aquatic and terrestrial stages are connected by a short metamorphic phase that dramatically restructures the body. The exploitation of available food resources, with moderate probability of mortality in two different life phases, can be considered the primary advantage of a complex life cycle (Harris 1999 and references therein). It is common in the literature to label tadpoles as herbivorous, because many species take up algae and other plant materials, but the true food items that tadpoles ingest and assimilate across taxonomic groups have not been investigated on a broad scale (Altig et al. 2007). Some studies suggest that animal matter and predation play a more important role in tadpole feeding and that tadpoles occupy a higher level in the aquatic food web than previously thought (Petranka and Kennedy 1999; Vera Candioti 2007). Because tadpoles with beaks and keratodonts are often observed eating dead siblings or carrion in laboratory and natural settings, it is suspected that many supposedly herbivorous species may turn out to be opportunistic omnivores upon closer investigation (McDiarmid and Altig 1999; Altig et al. 2007). Food items usually are small, generated with larval beaks or not, and are flushed into the mouth with water current produced by the hyal pumping mechanism (de Jongh 1968; de Jongh and Gans 1969; Gradwell 1972). In the bucco-branchial cavity, branchial filter epithelia and mucus secretions trap the food items (Dodd 1950; Kenny 1969). The presence of mucus entrapment and facultative suspension feeding is considered apomorphic for the Anura (Sokol 1975; Haas 2003). This food entrapment and filtering allows the exploitation of a wide variety of food resources from small, unicellar organisms, floating algae, bacteria, and fungi, to rasping leaves, feeding on carrion, and sifting through detritus at pond bottoms (Altig et al. 2007).

Obligate or high degrees of carnivory, herein defined as feeding exclusively or predominantly on metazoan food sources, have been confirmed only in tadpoles of a few frog genera (Altig and McDiarmid 1999). Carnivorous tadpoles that engulf large food items in toto have been classified macrophagous (Altig and Johnston 1989) or megalophagous (Ruibal and Thomas 1988). We prefer the former term, implying an uptake of food items that are significantly larger than food items in generalized opportunistically feeding tadpoles and large relative to the tadpole's own size. Macrophagy and carnivory have each been used to define tadpole guilds (Altig and Johnston 1989), despite the independence of these terms (size vs. kind of food). In most known cases, macrophagous tadpoles are carnivores, but macrophagy can be combined with herbivory (macrophagous herbivore) if large plant parts are swallowed as suggested for some *Dendropsophus* (Wassersug 1980). Herein, we use carnivory as an inclusive category for both macrophagous carnivores and carnivores that are not macrophagous.

Obligate carnivorous tadpoles are rare. The macrophagous carnivorous larva of the Neotropical *Lepidobatrachus* species (Ceratophryidae) is a suction feeder that can engulf and swallow large prey, such as tadpoles of other species and conspecifics (Cei 1968; Ulloa Kreisel 2002; Fabrezi and Lobo 2009). Related to this mode of feeding, and in contrast to almost all other anuran larvae, the snout is very broad and the oral orifice is wide in larval *Lepidobatrachus*; beaks are reduced, and keratodonts are absent (Ruibal and Thomas 1988; Altig and Johnston 1989; Haas 2003). Additionally, derived anatomical character states related to this mode of feeding can be identified in the cranium, musculature, buccal structure, and gut of this species (Ruibal and Thomas 1988; Lavilla and Fabrezi 1992; Haas 2003; Vera Candioti 2007; Fabrezi and Quinzio 2008; Ziermann et al. 2011). The closely related *Ceratophrys cranwelli* and *C. ornata* have carnivorous larvae as well, but they actively attack tadpoles of sympatric species by holding their prey with their mouthparts and biting off flesh. Their jaw and hyoidean musculature are strongly developed (Vera Candioti 2005; Fabrezi and Quinzio 2008; Natale et al. 2011). Independent evolution of masticatory carnivorous feeding, accompanied by large larval beaks bearing projections, hypertrophied jaw muscles, and predatory behavior, has been documented in *Hoplobatrachus* (Grosjean et al. 2004) and *Spea* (Bragg 1956, 1964; Fox 1990; Pfennig 1992). Interestingly, tadpoles of the genus *Spea* are facultatively carnivorous, where the presence of fairy shrimp early in premetamorphosis induces a carnivore morph characterized by not only larger jaw muscles and altered larval beak shape but also larger overall body size, shorter intestine length, and shorter larval period (Pomeroy 1981; Pfennig 1992). Macrophagous larvae of the *Dendropsophus microcephalus* group (some species have herbivorous and some have carnivorous larvae) have moderate jaws and lower lips that form a suction tube (Wassersug 1980; Vera Candioti et al. 2004; Vera Candioti 2007).

Tadpoles of *Hymenochirus*, and presumably *Pseudohymenochirus*, demonstrate a unique form of carnivory that involves biomechanics convergent with teleosts to create suction for feeding upon small live prey (Sokol 1962; Deban and Olson 2002). Oophagy as another form of carnivory has been reported from pond species (Petranka and Kennedy 1999) and phytothelm-breeding species; in some of the latter, nutritive unfertilized eggs from the mother are consumed by offspring (Crump 1992; Jungfer 1996). Reduction in intraoral epithelial structures, such as branchial food traps and filter rows, has been reported in the carnivorous larva of *Dendropsophus*, *Lepidobatrachus laevis*, and *Ceratophys* species (Wassersug 1980; Wassersug and Heyer 1988; Haas 2003; Vera Candioti et al. 2004; Vera Candioti 2005).

In this work, we present evidence that the tadpole of the Bornean Seep Frog, *Occidozyga baluensis* (Dicroglossidae), possesses a macrophagous carnivorous tadpole with many, to our knowledge, autapomorphic features. *Occidozyga* is an Asian member of the Dicroglossidae. We present field-based observations and anatomical evidence to address the questions related to the extent of carnivory in this species and the anatomical features that relate to this feeding mode. Examination of structurally and ecologically extremely aberrant tadpoles (see Haas et al. 2006) has the potential to change our perception of tadpole morphospace (Roelants et al. 2011) and lets us better understand the diversification processes in anuran evolution.

Materials and methods

Specimens examined

Tadpoles of *O. baluensis* (Boulenger 1896) (Table 1) were collected from Gunung Mulu National Park (Sarawak, Malaysia; N04°02.166′; E114°49.588′; 36 m asl) and Gunung Kinabalu National Park (Sabah, Malaysia) on March 25, 2009 (field no. #492; Table 1), and August 22, 2007 (field no. #439), respectively. Tadpoles and adults were identified by earlier published descriptions (Inger 1985; Boulenger 1896; Malkmus et al. 2002; Inger and Stuebing 2005). Genetic barcoding (16S mtDNA) facilitated the matching of larvae to adults from syntopic areas. Genetic sequences from adults and larvae were 99 % (#492) and 100 % (#439) identical. Tadpoles #439 were collected at night from a leaf litter filled, flooded depression in the forest floor, whereas #492 was collected from a shallow, approximately 3 m^2 (0–30 cm deep), silty-bottom puddle on a forest trail, containing some leaf litter. Several tadpoles from each sample were photographed (Nikon D80/D90, Micro Nikkor 2.8/105 mm, multiple flashes; Fig. 1). Sample #492 was kept alive in the field for 2 days in a

Table 1 Materials examined of *Occidozyga baluensis* larvae examined

Field/lab number	Catalog	Head-body length in mm	Preparation/remarks
#492P	ZMH A 13117	–	None; photos of living specimen
#492-1	ZMH A 13112	6.05	Histological serial sections
#492-2	ZMH A 13111	6.15	Histological serial sections
#492-3	ZMH A 13113	5.63	Histological serial sections
#492-4	ZMH A 13118	6.37	Histological serial sections
#492-5	ZMH A 13114	6.60	Histological serial sections
#492-6	ZMH A 13110	6.18	Histological serial sections (Morphisto GmbH), 3D reconstruction
#492-7	ZMH A 10851	5.50	Alcian stain, manual dissection
#439F	ZMH A 09367	–	Lot; several specimens
#439-1	ZMH A 13115	4.10	µCT scan, iodine impregnated
#439-2	ZMH A 10853	6.22	Cleared and stained; beetle larvae
#439-3	ZMH A 10854	6.73	Cleared and stained; beetle larvae
#439-39/01	ZMH A 10852	8.38	Cleared and stained

Because the Gosner (1960) staging table was not suitable for this species, we give head-body length. The largest specimen is fully grown and may be approximately equivalent to Stages 39–40 in the Gosner table

plastic box together with several tadpoles of *Ingerophrynus divergens* and *Rhacophorus pardalis* from the same puddle. Feeding observations were made in this setting (Fig. 2a, b). Tadpoles were euthanized in 2 % chlorobutanol and preserved in the field in 4 % neutral buffered formalin after these observations. Due to aberrant developmental patterns of hind limbs (see below), the commonly used staging table of Gosner (1960) is of limited use to estimate larval developmental stages of this species.

Histology, µCT, and 3D reconstruction

Six specimens were decalcified (Dietrich and Fontaine 1975), embedded in paraffin, and cut at 6–8 µm thickness (general protocols in Mulisch and Welsch 2010) on a Microm HE 340E semi-automatic rotary microtome or were re-fixed in Bouin solution, paraffin-embedded, and cut by a commercial provider (Morphisto GmbH, Frankfurt) at 6 µm thickness. Sections were stained either
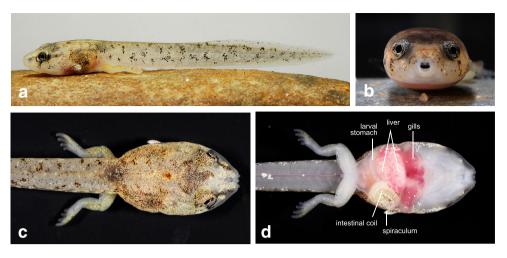
Fig. 1 Larval *Occidozyga baluensis* (#492P; ZMH A 13117) in life. **a** The lateral view shows fins restricted to posterior half of tail; hind limbs well developed (in all specimens collected). **b** The frontal view shows horseshoe-shaped lips of anteriorly directed, rounded oral orifice. Also, the frontal view reveals that eyes are directed anteriorly and that stereoscopic vision is likely. **c** In dorsal view, well-developed hind limbs, eye axis orientation, short snout, and spiracular siphon (left side of body) are clearly visible. **d** The ventral view shows large size of liver (identifiable as a *pale red* organ posterior to *bright red* gill region)

Fig. 2 Evidence of dietary habits of *Occidozyga baluensis*. **a** *O. baluensis* tadpole (unidentified specimen from lot, #492) attacking and feeding on tail of a *Rhacophorus pardalis* larva. Both specimens were collected from the same puddle and kept alive in a plastic container for several hours during which the attack occurred. **b** Body remains of the *R. pardalis* tadpole after attack. At the end of the tail, soft tissues have been devoured by the predating *O. baluensis* and the notochord (*arrow head*) remains. **c** Dissected *O. baluensis* (ZMH A 10854) larva showing large stomach-like extension of the gut. **d** Same specimen, beetle larvae removed from gut of tadpole

following our custom Azan protocol or Masson–Goldner–Trichrome (Mulisch and Welsch 2010). Covered slides were then scanned digitally with a Leica DM 6000 B microslide scanner microscope. Digital images were processed (sharpening, cropping, tonal range) with Adobe Photoshop®, Apple Aperture™, and Nik Silver Efex Pro™.

Three specimens were subject to the clearing and staining protocol (Dingerkus and Uhler 1977) as modified by Taylor and van Dyke (1985). One of the specimens was stopped after the initial alcian blue staining and transferred to 70 % ethanol for manual dissection of the musculature under a stereomicroscope (Leica). One specimen was transferred to distilled water; every step (70, 50–30 % EtOH) was maintained for 24 h. The specimen was impregnated with iodine solution following the protocol suggested by Metscher (2009). High-resolution, synchrotron-based X-ray CT imaging was performed at Beamline W2 (maintained by the GKSS research center, Geesthacht) of the DORIS III accelerator ring at the German Electron Synchrotron (DESY) in Hamburg, Germany. The specimens were scanned with a 30-keV X-ray beam. X-ray images were captured over a rotation of 360°. The resulting X-ray dataset was converted to a VGStudio Max (Volume Graphics GmbH, Heidelberg, Germany) volume dataset and exported as a single binary file (extension.dat) that contained all the raw image information.

Two 3D reconstructions were made: (1) from the digitized stack of histological sections (specimen ZMH A 13110) and (2) from the μCT volumetric dataset (ZMH A 13115; Fig. 3). Each was processed and segmented with AMIRA® software (Visualization Science Group). In the histology stack, muscles, bones, and cartilages of the head were segmented, whereas in the μCT stack cartilages, muscles, brain, eyes, and gut (not all shown herein) were segmented. In case of the histological image stack, polymesh surfaces were exported from segmented objects, each in separate.obj files. These files where imported into MODO® 701 (Luxology) 3D visualization software, reduced in polygon count, and used as 3D backdrops for remodeling. The export of polymesh surfaces from volumetric datasets produced some artifacts: (1) very small openings, such as the foramen trochleare and foramen craniopalatinum, were not retrieved after export; the openings became occluded in the process and (2) because the transformation algorithm has to set a threshold; polymesh surfaces were slightly inflated causing surface overlap in closely structures (for example, palatoquadrate–ceratohyal articulation). These artifacts were corrected manually as carefully as possible.

Coloration, shading, textures, and muscle fiber look in the 3D models are not meant to replicate actual tissue properties, but rather to facilitate visual anatomical understanding. General muscle fiber orientation for each of the muscles was confirmed by dissection of specimen ZMH A10851 and drawn by hand onto each of the muscles displacement map (see MODO 701 user manual). The displacement map was also taken as group mask to give more elevated fibers a different coloration to increase the fiber effect. We chose colors, transparency settings, subsurface scattering, and textures in such a way that textures resemble cleared and stained (cartilage, bones) or dissected specimens (muscles). The aim was to facilitate quick comprehension of visual representations for those experienced in these common types of preparation. Renderings of various views were performed with environmental lighting scheme in MODO 701. A virtual focal length of f 100 mm was set to the render camera, except if otherwise mentioned. Work in MODO 701 was done following standard manuals (e.g., Ablan 2008).

Homologies and terminology

Criteria of homology assessment applied herein focus on primary homology assessments (de Pinna 1991; Brower and Schawaraoch 1996; Richter 2005) such as topological relations and/or connectivity in the context of other structures (e.g., muscle origin and insertion sites). In many cases, homologies (equivalent structures) were obvious in comparisons with other taxa, yet in some cases, a hypothesis of homology had to be formulated. We consider muscles to be topographically identical and homologous (i.e., a primary homology; Rieppel and Kearney 2002) if they are similar in form (origin or insertion, and position relative to other muscles and skeletal structures) and if they pass the conjunction test (i.e., multiple homologs may not exist in the same organism; Patterson 1982). In this study, we do not consider secondary homologies formally because we did not perform a phylogenetic analysis.

We use anatomical terms for skeletal structures in the tradition of Gaupp (1893, 1894) and de Jongh (1968), preferably in Latinized form, to designate their nature as defined technical descriptors; comprehensive compilations of anatomical terms for anuran tadpoles are available elsewhere (Haas 2003; Roček 2003). We follow muscular terminology that has been discussed and justified (with respect to homology) for amphibians in previous studies (Haas 1997, 2003; Haas et al. 2006; Kleinteich and Haas 2006, 2011). Taxonomic names were mostly drawn from Frost (2013), but for higher taxa, we also adopted names from Pyron and Wiens (2011).

Morphological descriptions

The descriptions of the cranium, the musculature, and intestinal tract are based on specimen ZMH A 13110 and ZMH A 13113, if not otherwise stated, but no deviation in
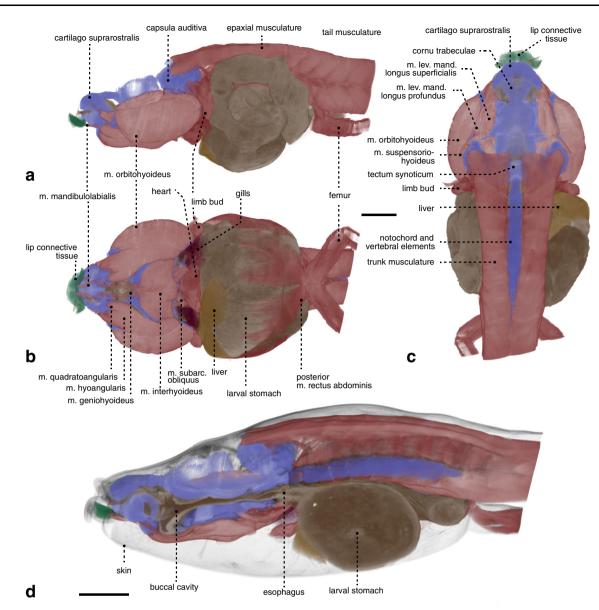
Fig. 3 Renderings of segmented, volumetric representation of the µCT dataset (ZMH A 13115); cartilages: *blue*, muscles: *red*, bones: *white*, gut: *olive*, connective tissue: *green*, and skin: *gray*. Anterior to the left, except for **c**: to the top. **a–c** lateral, ventral and dorsal views, respectively. The µCT data are in accord with findings from serial histological reconstruction (Figs. 4, 5, 6). In addition, it shows qualitative features were found in other specimens examined (Table 1), except for the extent of bone growth, particularly the size and position of the gut. A larval stomach is formed in *Occidozyga baluensis*. **d** Sagittal cross section through volumetric dataset including skin representation. The size of the stomach relative to other structures is evident in cross-sectional view. *Scale bars* 0.5 mm

qualitative features were found in other specimens examined (Table 1), except for the extent of bone growth, which, of course, relates to larval size and age. Rather than present a lengthy description of all cranial features, we provide an abbreviated description with annotated illustrations (Figs. 4, 5, 6, 7) and focus descriptive efforts on those features in which *O. baluensis* is unusual or diverges from other known ranids. Foramina, eye muscles, and ossifications will be neglected. Highly detailed descriptions of tadpole cranial structures are available elsewhere (e.g.,

Gaupp 1893, 1894; de Beer 1937; de Jongh 1968; Haas 2003; Roček 2003).

Results

External morphology

A thorough description of the external larval morphology of *O. baluensis* is available (Inger 1985) and is thus illustrated
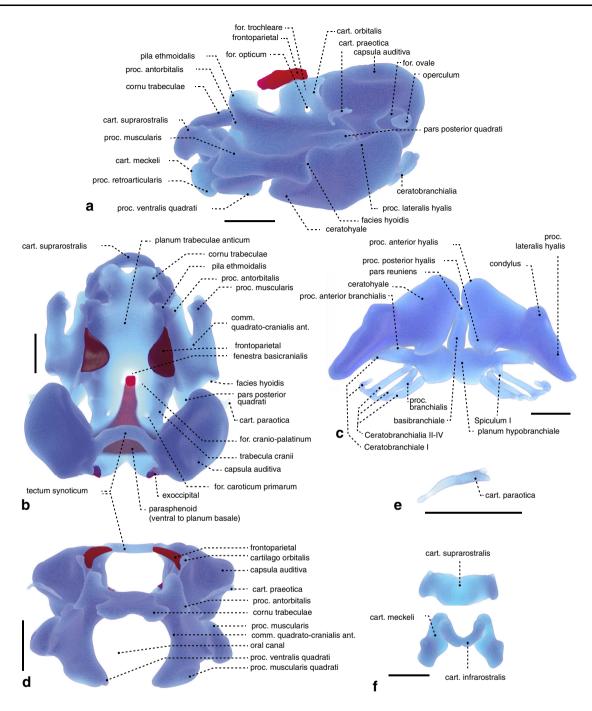
Fig. 4 *Occidozyga baluensis* larval cranium. 3D visualization based on a reconstruction of serially sectioned specimen (ZMH A 13110), cartilage: *blue* and bone: *red*. **a** Lateral view of the cranium, anterior to the left. The cranium of *O. baluensis* has a short snout (cornu trabeculae). The jaw cartilages are strong. The posterior cartilago orbitalis and the operculum are well developed. The ceratohyale is exceptionally large. A unique cartilago praeotica is located right anteroventral to the anterior cupula of the capsula auditiva. This cartilage has no confluences to other cartilages. **b** Dorsal view shows in particular the unique configuration of the palatoquadrate, its processus muscularis, and its lack of a fenestra suborbitalis. **c** The

dorsal view of the isolated hyobranchial apparatus shows the proportionately large size of the ceratohyale and the small size of the caudal visceral arch structures; the Ceratobranchiale I is reduced and only present with proximal and distal rudiments. **d** frontal view of the neurocranium and bones showing the rounded canal formed by cornua trabeculae dorsally and palatoquadrate laterally; it also shows the position of the cartilago praeorbitalis. **e** isolated right cartilago praeotica, frontal view; **f** upper and lower jaw cartilages spread apart to show both, frontal view. *cart.* cartilage, *for.* foramen, *proc.* processus. *Scale bars* 0.5 mm
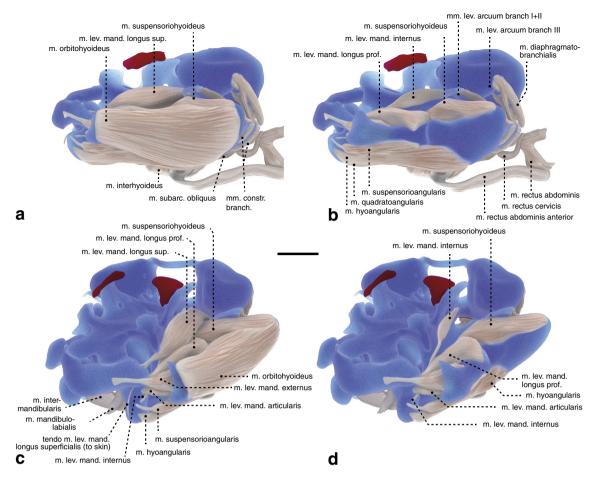
Fig. 5 *Occidozyga baluensis* larval cranium and cranial muscula-ture. 3D visualization based on a reconstruction of serially sectioned specimen (ZMH A 13110); cartilage: *blue*, bone: *red*, and muscle: *whitish brown*. Cranial musculature was reconstructed on the left side only. **a**, **c** Lateral and anterolateral views, respectively, of the cranium, anterior to the left. The cranial musculature of *O. baluensis* is dominated by the enormous m. orbitohyoideus. The very flat m. abdominis anterior appears stronger than it is in this perspective because of its orientation toward the camera. **b**, **c** In these visualizations, the m. orbitohyoideus, m. lev. mand. externus, and m. lev. mand. longus superficialis were hidden to expose other muscles. *m.* musculus, *lev.* levator, *mand.* mandibulae, *prof.* profun-dus, **b** and **c** were rendered with 50 mm virtual focal length. *Scale bar* 0.5 mm

herein without repeating a general external morphological description (Figs. 1, 2). With regard to feeding, however, it is worth pointing out the anteriorly directed eyes, and the padded, horse-shoe-shaped ventral lip and reduced upper lip (flap) that both lack keratodonts (Fig. 1b, c). The hind limb development is exceptional: All specimens collected, regardless of body size (Table 1), had well-developed hind limbs. CT scanning revealed divergent development of fore and hind limbs (Fig. 3) in specimen ZMH A 13115, which was the smallest and presumably youngest individual in the series. Its hind limbs were at Stage 38 according to the standard staging table of Gosner (1960), whereas the fore limbs corresponded to approximately Stage 31 of limb development. Similarly in cleared specimens (ZMH A 10853–4, Table 1), hind limb ossification corresponded to Stage 40 and fore limb approximately to Stage 36 in other species (Haas 1999) with significant size difference. In many neobatrachian tadpoles, Stage 40 hind limbs are indicative of mid-metamorphosis specimen, but the much less developed fore limbs suggest that the individuals were not in metamorphosis.

Cranial skeleton

The cornu trabecula is very short, accounting for ca. 16 % of the total cranial length. The cornua diverge only in the distal forth of their lengths. Posteriorly, they are confluent with the planum trabeculare anticum. Posterior to the latter, the cranial base is almost completely covered by cartilage. The remnant of the fenestra basicranialis between the trabeculae cranii is small and restricted to an area just dorsal to the anterior tip of the parasphenoid (Fig. 4b); the fenestra is devoid of cartilage but spanned by collagen-rich tissue. On each side of the fenestra bas-icranialis, a foramen craniopalatinum pierces the cranial floor. The processus antorbitalis projects laterally from the
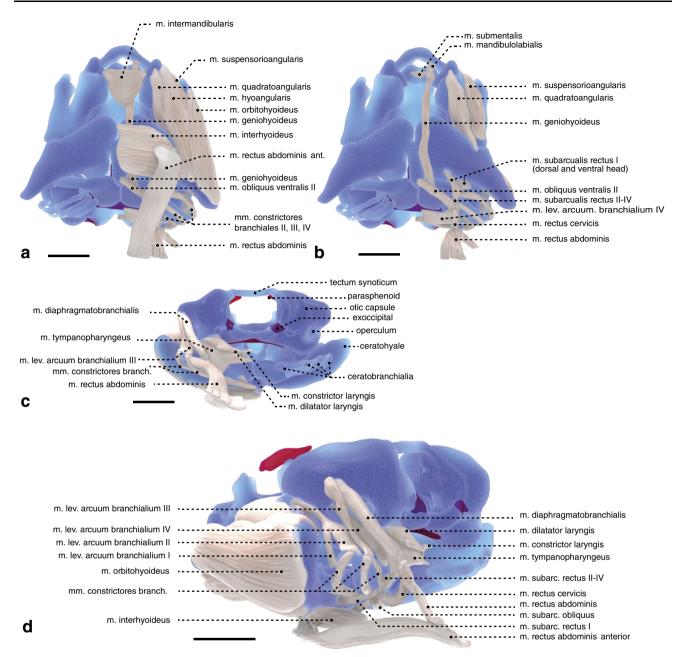
Fig. 6 Cranium and cranial musculature in ventral views. 3D visualization based on a reconstruction of serially sectioned specimen (ZMH A 13110), cartilage: *blue*, bone: *red*, and muscle: *whitish brown*. **a** The superficial layer shows large muscles (both in length and diameter) of the angularis group and the broad m. interhyoideus. The m. rectus abdominis anterior is an unusual feature in tadpoles and developed as a thin band (attaching to ventral skin and via a tendon to the ceratohyale). **b** Same view but m. intermandibularis, m. interhyoideus, and m. rectus abdominis anterior have been removed to expose hidden deeper layer muscles. **c** posterior view, complete set of muscles; **d** posterolateral view to show more details of the branchial levator and constrictor groups; complete set of muscles. *cart.* cartilage, *m./mm.* musculus/musculi, *proc.* processus. *Scale bars* 0.5 mm

planum trabeculare anticum. Dorsally, two conspicuous pillars arise from the planum trabeculare anticum: the pilae ethmoidales, situated posterior to the nasal organ. The pila ethmoidalis also contributes to the lateral wall of the braincase, i.e., the cartilago orbitalis. In general, the cranial sidewall is very well developed, however, its anterior (pila ethmoidalis) and posterior parts (cartilago orbitalis proper) are separated by a deep cleft (Fig. 4a). The cartilago orbitalis is not fused to the capsula auditiva (Fig. 4b). The otic capsule is relatively large, comprising 40 % of total cranial length. The operculum is present and large (Fig. 4a). The tectum synoticum connects the otic capsules, but taenia tecti transversalis and taenia tecti medialis are absent.
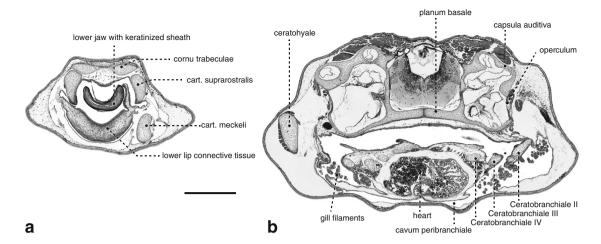
Fig. 7 Digital photographs of transverse sections through specimen ZMH A 13110, same scale. **a** The cross section at the level of the posterior portion of the upper jaw (cart. suprarostralis) and anterior part of the lower jaw shows the thick, padded lower lip; the lower lip tissue stains densely for collagen fibers but does not show cartilage cells. **b** Cross section through the branchial region to show that epithelial filter structures are absent dorsal to the ceratobranchialia; gill filaments are present below ceratobranchialia in peribranchial chamber. Original *color* scans from slide scans were transformed to halftones, background was removed, tonal range adjusted, and images were slightly sharpened. *Scale bar* 0.5 mm

The cartilago suprarostralis (=cartilago labialis superior, Gaupp 1894) is undivided and strongly developed (Fig. 4f). It is a broad-arched band of cartilage with dorsal articulation to the cornu trabeculae. Lateral to the articulation, a knob is formed (Fig. 4a, f). The ventral margin of the cartilago suprarostralis is softly emarginated laterally; thus, the medial parts project further ventrally. A clear distinction of the suprarostral pars alaris and pars corporis as in many other tadpoles (Haas 2003) is not possible. The lower jaw is a continuous cartilage body forming two functional segments: the cartilago meckeli laterally and the cartilago infrarostralis medially (Fig. 4f). The S-shape and processes of the cartilago meckeli conform with those of other tadpoles; however, it deviates from the expected general pattern in which it is relatively long and its major axis is oriented mostly dorsoventrally in anterior view (Fig. 4f), rather than more obliquely or horizontally.

The anatomy of the palatoquadrate is unique. It is positioned laterally to the neurocranium slightly below the level of the trabecula cranii and in an approximately horizontal position. There is only one very broad connection of the palatoquadrate to the trabecula cranii. We homologize this broad connection with the commissura quadrato-cranialis anterior and claim that the processus ascendens (posterior connection of the palatoquadrate) was lost (see discussion), resulting in the absence of a fenestra subocularis.

The processus oticus quadrati (connection to crista parotica) is absent; however, a more medial, broad projection of the palatoquadrate extends toward the capsula auditiva ventral to its anterior bulge (cupula anterior);

descriptively, we name this the pars posterior quadrati. Dorsal to this projection and just anterior to the cupula anterior, there is another cartilage isolated from surrounding cartilages. To our knowledge, an isolated cartilage in front of the capsula auditiva has not been reported in tadpole skulls; we therefore describe it here as the cartilago praeotica (Fig. 4). The most plausible assumption of homology based on position and connection to musculature (see below) is that this cartilage is palatoquadrate material and homologous to the curvatura posterior quadrati in other tadpoles (Haas 2003).

The remainder of the palatoquadrate comprises two more major areas. First, a strut of cartilage is horizontal in orientation, is directed anteriorly, and is unlike any other palatoquadrate structure we know. Because of its position and muscle attachments (see below), we apply the term processus muscularis, implying homology to structures of the same name in other taxa. Second, the pars articularis quadrati runs anteroventrally from the main body of the palatoquadrate and establishes articulation with the lower jaw. The medial edge of the pars articularis quadrati is extended posteriorly and ventrally and forms a structure that we choose to name processus ventralis quadrati (Fig. 4a). In anterior view (Fig. 4d), it is obvious that the robust cartilage tissues of pars articularis, processus ventralis, commissura quadrato-cranialis anterior, and cornu trabeculae almost completely encircle a space for the anterior alimentary canal, hereafter, the oral canal (Fig. 4d).

Another unique feature of the palatoquadrate is its articulation with the ceratohyale. The articulation is located far posteriorly, behind the center of the eye (not shown but

part of the CT dataset). Furthermore, the articulation (facies hyoidis; Fig. 4a, b) is not oriented ventrolaterally as in most other tadpoles but faces posteriorly, forming a deep emargination of the palatoquadrate's lateral margin.

The hyobranchial apparatus is dominated by the huge ceratohyalia (Fig. 4c). These are massively built cartilages with a horizontal medial part bearing the processus anterior and posterior hyalis, and a lateral, more vertical processus hyalis lateralis. Anteriorly, the processus lateralis hyalis bears the condylus for articulation with the palatoquadrate. Both ceratohyalia are connected medially by the pars reuniens, which is posteriorly confluent with the basi-branchiale. Synchondrotic articulations connect the basi-branchiale to the planum hypobranchiale posteriorly. The planum hypobranchiale is relatively small in area. It gives rise laterally to Ceratobranchiale I, which terminates laterally in a blunt end and is disconnected from what appears the distal part of the Ceratobranchiale I (Fig. 4c). At the proximal base of Ceratobranchiale I, there is a posteriorly projecting spur that we homologize with Spiculum I. The tissue around the glottis is dense, but has not chondrified in the specimen used for 3D reconstruction (present in a pre-cartilaginous tissue stage in ZMH A 13113). Ceratobran-chialia II–III are shallowly arched (dorsoventrally) simple rods. Distally, they are confluent via commissurae termi-nales. In Ceratobranchiale III, a ventral thickening, the processus branchialis, is present (muscle attachment site, see below).

Cranial musculature

The origins and insertions of cranial muscles are presented in Table 2.

The levator mandibulae group (Fig. 5; nervus trigemi-nus innervated) is composed as usual of the following: mm. levatores mandibulae longus superficialis, lev. mand. lon-gus profundus, lev. mand. internus, lev. mand. externus, and lev. mand. articularis. In reconstructions, a m. levator mandibulae externus superficialis was not clearly separate from a m. lev. mand. externus profundus. We do not make the distinction here, although some dorsal fibers resembling a m. lev. mand. superficialis are discernible in histological sections where they are seen as fibers that originate slightly more anteriorly than the bulk of the externus fibers. The m. lev. mand. lateralis is absent in the specimens examined. The levator muscles present some unusual features. First, the m. lev. mand superficialis reaches posteriorly beyond the palatoquadrate and originates ventromedially at the otic capsule and adjacent planum basale. It is a thick muscle that covers the thin m. lev. mand. internus medial to it. Anteriorly, the tendon of the m. lev. mand. longus super-ficialis attaches in the common pattern to the processus dorsomedialis of the cartilago meckeli, but also produces

an atypical ventrolateral branch whose tendon runs between the upper and lower jaw cartilages and connects to the skin anterior to cartilago meckeli (Fig. 5c). The m. lev. mand. internus has relatively short fibers, ending in a long tendon (Fig. 5d). The m. lev. mandibulae articularis crosses the tendon dorsally, and the two muscles insert close to each other on the lateral aspect of cartilago meckeli. The m. lev. mand. externus and m. lev. mand. longus profundus have separate insertions at the cartilago suprarostralis. Both muscles are very thick in diameter. The m. lev. mand. externus fills most of the gap between pro-cessus muscularis and processus articularis quadrati; the m. lev. mand. longus profundus reaches far back onto the pars posterior quadrati and the area anterior to the articulation with the ceratohyale (Fig. 5b, d). The additional mandib-ular muscles (m. intermandibularis, m. submentalis, and m. mandibulolabialis) all present typically in this taxon.

Six muscles are associated with the second visceral arch: m. interhyoideus, m. hyoangularis, m. quadratoangularis, m. suspensorioangularis, m. orbitohyoideus, and m. sus-pensoriohyoideus (Figs. 5, 6). It is noteworthy that m. in-terhyoideus and the angularis-group muscles are unusually well developed and have large cross-sectional areas. Additionally, the angularis-group muscles are more elon-gate than typically found in ranid tadpoles, due to the posterior position of the ceratohyale.

The m. orbitohyoideus is enormous, both in length and diameter, dominating the skull in lateral view (Fig. 5a). The fiber orientation is unusual because fibers run almost hori-zontally. The m. suspensoriohyoideus is typically in close association with the former and insertion on the processus lateralis hyalis. The transverse orientation of m. suspenso-riohyoideus and origin from the pars posterior quadrati (Fig. 5c, d) is to our knowledge unique among tadpoles (origin from posterior proc. muscularis in other taxa).

In anuran larvae, the branchial section typically com-prises several muscle groups: branchial levators, constric-tors, and subarcual muscles; laryngeal muscles (m. dilatator laryngis and m. constrictor laryngis); and spinal muscles (m. geniohyoideus, m. rectus cervicis, m. rectus abdominis, and m. diaphragmatobranchialis) (Figs. 5, 6). In *O. baluensis*, most of these muscles are located as is expected. A m. interhyoideus posterior is missing. The m. diaphragmatobranchialis originates from the "diaphragm" (tissue separating posterior gill chamber wall and anterior abdominal wall) and inserts on the lateral semicircular canal of the capsula auditiva, next to the m. levator arcuum branchialium III (insertion in other taxa typically distal end of Ceratobranchiale III). The m. rectus abdominis inserts to the diaphragm form the posterior, close to the m. dia-phragmatobranchialis' origin (Fig. 6b, c). In proximity to the attachments of m. rectus abdominis and m. diaphrag-matobranchialis, the m. rectus cervicis originates on the

Table 2 List of cranial muscles and their origin and insertion sites in *Occidozyga baluensis*

Musculus	Origin	Insertion	Comment
Mandibular group, n. trigeminus (c.n. V) innervated			
Levator mandibulae longus superficialis	Ventromedial face of anterior capsula auditiva and adjacent planum basale; pars posterior quadrati	Tendon bifurcates distally: superior slip inserts onto the processus dorsomedialis of cartilago meckeli; inferior slip runs between cartilagines suprarostrales and meckeli to insert in soft tissue lateral of the lower lip	
Levator mandibulae longus profundus	Dorsally and laterally on palatoquadrate body, anterior to articulation with ceratohyale	Ventromedial aspect of posterior tip of cartilago suprarostralis	Insertion not joining tendon of levator mandibulae externus
Levator mandibulae externus	Anteromedial part of processus muscularis	Relatively long tendon attaches to anterolateral aspect of the cartilago suprarostralis	An anterior and dorsal fiber group of the externus probably corresponds to the externus superficialis in other species but is not separate from the remainder at insertion; tendon not joined by levator mandibulae longus profundus
Levator mandibulae articularis	Dorsolateral surface of the palatoquadrate opposite of the processus muscularis	Dorsolaterally at cartilago meckeli	This muscle is deep to mm. levatores mandibulae longus et externus, but superficial to the tendon of the m. lev. mand. internus
Submentalis (syn.: intermandibularis anterior)	Ventrally on cartilago infrarostralis, in the symphyseal region	Arching from one side to the other	
Intermandibularis	Median raphe	Ventromedial face of cartilago meckeli	Thin muscle with loose fibers has a very posterior slip that may extend to the area near the anterior tip of the ceratohyale
Mandibulolabialis	Medial face of cartilago meckeli at base of processus dorsomedialis	Ventrolateral corners of lower lip	
Levator mandibulae internus	Lateral wall of the neurocranium (trabecula cranii), posterior to the foramen oculomotorius	Crosses deep to all other mandibular levators with long tendon laterally and inserts on the lateral part of cartilago meckeli	
Hyoid group, n. facialis (c.n. VII)			
Hyoangularis	Anteroventral aspect of ceratohyale, ventral to its condylus	Broadly at processus retroarticularis of cartilago meckeli	
Quadratoangularis	Ventral surface of palatoquadrate just anterior to the ceratohyale–palatoquadrate articulation	Retro-articular process of cartilago meckeli, ventral to insertion of m. hyoangularis	
Suspensorioangularis	Posterior base of the processus muscularis of the palatoquadrate, just anterior to the ceratohyale–palatoquadrate articulation	Retro-articular process of cartilago meckeli, dorsal to insertion of m. hyoangularis	
Orbitohyoideus	Lateral and dorsal aspects of processus muscularis of the palatoquadrate	Broadly at processus lateralis hyalis	
Suspensoriohyoideus	Dorsal face of palatoquadrate body and pars posterior quadrati	Dorsally on posterior tip of processus lateralis hyalis, posterior and adjacent to m. orbitohyoideus	
Interhyoideus	Median raphe	Ventral surface of ceratohyale, approximately at parasagittal plane with condylus	

Table 2 continued

Musculus	Origin	Insertion	Comment
Branchial group, n. glossopharyngeus (c.n. IX) and n. vagus (c.n. X)			
Levator arcus branchialium I	Cartilago praeotica	Lateral portion of Ceratobranchiale I	Thin muscle from which lev. arc. branch. II diverges
Levator arcus branchialium II	Common origin on cartilage praeotica with levator arcus branchialium I	Terminal portion of Ceratobranchiale I and II, Commissura terminalis I	Branches off from the first branchial levator
Levator arcus branchialium III	From capsula auditiva dorsal of the foramen ovale	Commissura terminalis II between Ceratobranchiale II and III	
Levator arcus branchialium IV	From anterodorsal margin of foramen ovale on ventral surface of capsula auditiva	Terminal portion of Ceratobranchiale IV	
Tympanopharyngeus	Low, ventro-posteriorly from capsula auditiva, ventral to foramen perilymphaticum inferius	Sub-esophageal tissue, pericardium; processus branchialis III	Closely neighboring levator arcuus branchialium IV and difficult to delimitate from it
Constrictor branchialis I	–	–	Sensu Haas 1997; absent
Constrictor branchialis II	Proximal base of Ceratobranchiale I	Terminal commissure of Ceratobranchiale I and II	
Constrictor branchialis III	Anteriorly at proximal part of Ceratobranchiale III (processus branchialis)	Terminal commissure of Ceratobranchiale II and III	
Constrictor branchialis IV	Anteriorly at mid part of Ceratobranchiale IV	Terminal commissure of Ceratobranchiale II and III	
Subarcualis rectus I (dorsal head)	Lateral side at base of processus posterior hyalis	Base of Ceratobranchiale I, processus anterior branchialis	
Subarcualis rectus I (ventral head)	Ventral aspect of processus posterior hyalis	Ventrally from proximal Ceratobranchiale I and Ceratobranchiale III	
Subarcualis rectus II–IV	Ceratobranchiale IV	Processus branchialis of Ceratobranchiale III	Considering the insertion, this muscle could be called subarcualis rectus III–IV
Subarcualis obliquus II	Ventrally at posterior end of basibranchiale	Processus branchialis of Ceratobranchiale III	The processus urobranchialis to which this muscle usually connects is exceptionally flat in this species
Diaphragmatobranchialis	Diaphragm, i.e. connective tissue of joint post-branchial and pre-abdominal wall	Posteriorly at capsula auditiva at the level of the lateral semicircular canal	
Spinal group, spinal nerve innervation			
Geniohyoideus	Ventromedial at hypobranchial plate	Ventromedial aspect of cartilago infrarostralis in its posterior part	
Rectus abdominis	Abdominal wall	Diaphragm (see above)	
Rectus abdominis anterior	Diaphragm (see above)	To ventral skin (ventral to hyobranchial apparatus), with tendinous connection to ceratohyale, lateral to m. interhyoideus	
Rectus cervicis	Anterior continuation of m. rectus abdominis, originates broadly from abdominal wall (diaphragm)	Processus branchialis Ceratobranchiale III	

diaphragm and runs cranially to insert on the processus branchialis Ceratobranchiale III. The m. levator arcuum branchialium IV, m. tympanopharyngeus, and m. dilatator laryngis run proximate to each other. The m. tympanopharyngeus originates very low on the posterior end of the capsula auditiva floor, whereas the levator arcuum branchialium IV originates from the anterodorsal margin of the foramen ovale. The m. dilatator laryngis is

medial and posterior to the m. tympanopharyngeus; a small m. constrictor laryngis is positioned medial to the m. dilatator laryngis. A m. subarcualis obliquus IV is absent as in most tadpoles. The most unusual muscle in the branchial region is the m. rectus abdominis anterior. It extends the m. rectus abdominis (proper) anteriorly beyond the branchial diaphragm. It inserts to the ventral skin and with a tendon on the anteroventral face of the ceratohyale (Fig. 6a, d).

Anterior larval alimentary canal

The oral orifice is terminally positioned and bordered by a horseshoe-shaped lower lip. The lip is filled with dense, collagen-rich tissue giving it a padded appearance (Fig. 7a). The oral disc lacks papillae and keratodonts. Similar lip morphology in other species has been termed a suctorial tube (Lavilla 1990; Vera Candioti et al. 2004). Keratinized jaw sheaths are well developed both in the lower and upper jaws. In the region between the jaws and the ceratohyale, the ventral floor of the buccal cavity is formed like a pad in cross section and possesses medial tissue condensations and epithelial thickening reminiscent of a tongue anlage. Because the angle of the commissura quadrato-cranialis anterior is virtually vertical (Fig. 4d), buccal space is narrow between oral orifice and the hyal region. Buccal space moderately widens until the level of the hyal articulation, becoming significantly broader posterior to that level, at the transition to the branchial cavity.

In the branchial cavity, specialized filter epithelia (branchial food traps, secretory ridges) are absent and the ventral velum is reduced. Gill filaments are present (Fig. 7b). The glottis is directed anteriorly. The esophagus is short and begins under the roof of the planum basale. Its single-layer ciliated epithelium is rich in high columnar glandular cells and goblet cells. The esophagus narrows toward the level of the occiput and develops longitudinal epithelial folds ventrally. The posterior part of the esophagus is encircled by a tunica muscularis of smooth muscle fibers continuous with the same layer of the stomach. In general, there is only one relatively thick layer or collagen fibers (tela submucosa) deep to the lamina epithelialis of the esophagus and a muscularis mucosae was not discernible. The abrupt transition from esophagus to the larval stomach is left of the sagittal plane and at the transverse level of the occiput.

The anterior stomach epithelium consists mostly of columnar, ciliated mucus-producing cells, and glandulae gastricae with their secretory cells. We could not distinguish a cardia from a fundus section in our specimens. The tunica muscularis and tunica serosa are thin. In the anterior gastric section, glandulae gastricae are present ventrally and absent dorsally. Their epithelium is cuboidal and arranged around a central canal. In two specimens that we dissected, relatively large insect larvae (Coleoptera:

Elmidae and Scirtidae) were removed from the larval stomach (Fig. 2c, d). We saw insect larvae or cuticular debris in several other specimens either in histological section or through the translucent tissues of intact specimens.

In the posterior half of the larval stomach (Fig. 8), the glandulae gastricae invade the dorsal wall of the stomach as well, whereas ventrolaterally (right) glandulae gastricae already disappear to give way to the pyloric region with its folded tunica mucosa and underlying thick tunica muscularis. The small intestine leaves the larval stomach to the right. The intestine which is very short and coiled (Fig. 1d) had columnar cells with microvilli brush, an unusual highly folded lamina mucosa in the duodenal region, flattening out posteriorly.

The configuration of associated organs of the alimentary canal resembles the situation in adult ranids (Gaupp 1896): The three-lobed liver is large and occupies a significant portion of the abdominal cavity. The gall bladder is situated between the liver lobes and is also remarkably large. The pancreas is between the liver and the larval stomach (Fig. 8), and the ductus choledochus is embedded in it for most of its length. The pancreatic processus gastricus stretches dorsally over the full width of the stomach.
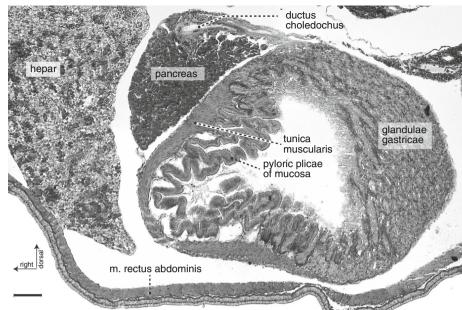
Discussion

Feeding

Based on our observations, we suggest that *O. baluensis* larvae are obligate carnivores: (1) the anteriorly directed mouth and horseshoe-shaped, cushioned lower lip are not suitable for scraping action, as in most other tadpoles; (2) filter epithelia that would trap fine food particles are absent in the branchial apparatus; (3) the ceratobranchialia and the branchial chamber are small in size and partially reduced (Ceratobranchiale I), whereas the ceratohyale is enormous in size; (4) the esophagus leads into a large larval stomach that contained whole insect larvae in some specimens; (5) eyes were anteriorly directed, likely allowing for stereoscopic vision; and (6) we observed feeding on other tadpole's tails. Furthermore, we suggest that this combination of characters does not allow for either substrate rasping or suspension feeding; we therefore conclude that the larvae of this species must be obligate macrophagous carnivores.

Although we observed the feeding on another tadpole's tail, the actual act of prey capture has not been recorded, and predation as well as predatory behavior by the larvae of this species needs further research. The round but relatively narrow terminal mouth, padded lower lip, and strongly supported oral canal (Fig. 4d) as well as the massively developed ceratohyal along with its strongly developed

Fig. 8 Histological section through the pyloric region of the larval stomach of *Occidozyga baluensis* (ZMH A 13118). The sections show several features of the larval stomach: its size, the relatively thick tunica muscularis of the pyloric region, the pyloric plicae of the mucosa to the left (right body side of specimen), and numerous glandulae gastricae in the right part of the image. The pancreas is adjacent but not connected to the larval stomach. Only one duct (ductus choledochus) could be detected that seems to carry both bile and pancreatic secretions. The duct enters the intestine posterior to the larval stomach. *Scale bar* 100 μm

musculature (m. orbitohyoideus, m. suspensoriohyoideus, and angularis group) strongly suggest that powerful suction is the key mechanism in food item uptake in *O. baluensis*. The suction feeding carnivorous tadpoles of *Hymenochirus boettgeri* are very small and predatory (Deban and Olson 2002). Like *O. baluensis*, *H. boettgeri* tadpoles are morphologically divergent from typical omnivorous tadpoles and lack a filter apparatus and scraping mouthparts; the eyes are large and frontally orientated. The feeding mechanism of *H. boettgeri* is similar to that of teleosts, in which it suction-feeds by using a combination of rapid mouth protrusion and hyobranchial depression. There are no keratinized mouthparts or strong upper jaw cartilages in *H. boettgeri,* and the lip is not padded as in *O. baluensis*. The anatomical features of *O. baluensis* do not suggest the same kind of protrusion of the mouth as in *H. boettgeri,* in which a U-shaped lower jaw opens the oral orifice rapidly. In *O. baluensis*, the cartilago meckeli is more dorsoventral in its main axis than horizontal as in most tadpoles, indicating that the mouth can open considerably when fully rotated out. Furthermore, the cartilago meckeli might rotate not only in the transverse axis but also in the longitudinal body axis, thus widening the lower jaw arch and allowing prey larger than the resting size of the mouth orifice (Fig. 1b); however, this needs to be tested. It would be concordant with the surprisingly large prey items we found in some of the larvae (Fig. 2d).

Rotation of the cartilago meckeli is a function of the exceptionally long angularis-group muscles (long fibers enable long distance of action and large ranges of articular rotation). *Hymenochirus boettgeri* utilize a mechanism to suck in food items generally smaller than its mouth (see illustration in Deban and Olson 2002), although it has been classified macrophagous in some studies (Satel and Wassersug 1981). This mechanism probably is different or at least not the only mechanism in *O. baluensis*. In *O. baluensis*, the sizes of prey items (Fig. 2c, d) can exceed the cross section of the mouth opening at rest. Thus, unlike in *H. boettgeri,* there might be several forceful gape cycles involved to fully engulf the prey. It seems likely that *O. baluensis* uses the lower lip to establish contact with prey and act as a sealing pad to apply strong suction and forcefully ingest prey through the oral opening and oral canal (Fig. 4d), but not necessarily with high speed. We suggest that the unusually thick diameter of m. orbitohyoideus and m. suspensoriohyoideus is an evidence of the ability to create these strong forces (Satel and Wassersug 1981). The separate insertions of the m. levator mandibulae externus and longus profundus on the cartilago suprarostralis might allow better control of the cartilago in prey contact than in other species where the two muscles share a common tendon (Haas 2001). Robust jaws and keratinized jaw sheaths are used to remove tissue from the prey, as supported by our observations (Fig. 2a, b). The large lumen of the larval stomach also supports the assumption that larvae consume food items so large (Fig. 2d) that tissue contact and even the stretching of mouthparts is necessary to engulf them.

The lower lip tube of *O. baluensis* has been described as "protrusive" (e.g., by Leong and Chou 1999), but the protrusive capabilities have not been documented. Based on our observations of anatomy, we can link protrusion

only to cartilago meckeli rotation. The cartilago meckeli is unusual in its dosoventral extent, and rotation of the cartilage would push the lower lip forward upon jaw opening (see Fig. 4f, mouth closed). Larval macrophagous carnivory (worms, insects) has been described for *O. sumatrana* tadpoles (Iskandar 1998), *O. lima*, and *O. laevis* (Smith 1916) and has been assumed for *O. baluensis* (Inger 1985) based on the reduced features of the oral and buccal cavities. Smith (1916) mentioned that *O. laevis* preyed on mosquito larvae and other small tadpoles as was documented herein for *O. baluensis*. Gut content analysis of *O. lima* and *O. laevis* in a previous study had failed to confirm macrophagy/carnivory (Heyer 1973).

Among the tadpoles described in the literature, *Dendropsophus nanus* (formerly *Hyla nana*; Hylidae) and *D. microcephalus* are strikingly similar in some features to *O. baluensis* (Vera Candioti et al. 2004; Vera Candioti 2007). Based on morphological characters and gut content analysis, these authors conclude that *D. nanus* has a macrophagous carnivorous tadpole with a likely preference for oligochaete worms. Features shared by the two species include the following: undivided cartilago suprarostralis, horseshoe-shaped lower lip (suctorial tube), absence of labial papillae and labial tooth rows, absence of pharyngeal epithelial filter structures, large ceratohyal area, long processus lateralis hyalis (lateral lever arm), small branchial basket area, reduced ceratobranchialia (first in *O. baluensis*, fourth in *D. nanus*), and large muscles in the depressor mandibulae group (particularly m. orbitohyoideus). The two species are well separated in the current phylogenetic system of the Anura (e.g., Pyron and Wiens 2011), and all similarities must be considered convergences and derived within their respective family, Dicroglossidae and Hylidae. Unlike *Occidozyga*, *Dendropsophus* species do not show the profound alterations of palatoquadrate structure (and concomitant unique muscle orientations), the accelerated hind limb development, and, although the branchial basket is small, all ceratobranchials are present in the latter (Vera Candioti 2007).

Hind limb heterochrony

All specimens examined and collected from various sites had well-developed hind limbs. Hind limbs were more advanced than fore limbs, more pronounced so than in other ranids (Haas 1999). The ontogenetic trajectory (growth/differentiation) of the limbs, however, could not be established in detail based on the limited materials. The accelerated growth of the hind limbs has been mentioned in *O. laevis* and *O. lima* (Smith 1916), as well as in *O. sumatrana* (Iskandar 1998). Early hind limb development is not exclusive to *Occidozyga* and has been reported in unrelated taxa such as *Indirana beddomii* (Veeranagoudar

et al. 2009) or *Arthroleptides martiensseni* (Drewes et al. 1989).

Smith (1916:174) reported on *Occidozyga lima* that "they have the habit of sprawling out their hind limbs in an ungainly manner, and of using them also as a means of locomotion, preferring to crawl slowly about by their aid, rather than use their tails." This is in accord with Heyer (1973) and our observations on *O. baluensis*, which remained motionless on the bottom of the pond for most of the time when observed (see also Pope 1931 for *O. lima* bottom-frequenting habits). Hind limbs may be functional early on in prey approaching behavior.

Digestive tract morphology

Consistent with its carnivorous diet, *O. baluensis* has digestive modifications seen in other carnivorous tadpoles. Among vertebrates, carnivores generally have a short intestine, whereas herbivores have long intestines relative to body length (Stevens and Hume 1995). *Euphlyctis hexadactylus*, the only known amphibian folivore, has relatively longer intestines and larger stomach, relative to the carnivorous syntopically occurring frogs (Das 1995). Similarly, frog species with carnivorous tadpoles have relatively short larval intestine length, as observed in *Ceratophrys* (Fry and Kaltenbach 1992; Fabrezi 2011), *Dendropsophus nanus* (Vera Candioti et al. 2004), carnivore morphs of *Spea* (Pfennig 1992; Storz and Travis 2007), *Lepidobatrachus* (Ulloa Kreisel 2002), and *Hymenochirus* (Hintze-Podufal and Schroer 1989). In contrast, the carnivorous tadpole of *Hoplobatrachus* may have an intestinal length not significantly different from omnivorous species (Grosjean et al. 2004). In *O. baluensis*, we observed a reduced number of intestinal coils (compared to herbivorous larvae), as also noted in *O. magnapustulosus, O. lima,* and *O. laevis* (Taylor and Elbel 1958; Heyer 1973).

The cross-sectional histology of herbivorous/omnivorous larval small intestines is a simple tube with a thin layer of mucosal cells, though some species have an infolding, called the typhlosole as in *Xenopus laevis* (Shi and Ishizuya-Oka 1996). This relatively simple intestinal structure is transformed to the carnivorous intestine of adult frogs, forming a trough–crest axis in cross section, analogous to the crypt–villus axis in mammalian intestines (McAvoy and Dixon 1977). Most carnivorous tadpoles examined have the simple larval intestinal histology that presumably transforms to the adult pattern during metamorphosis, such as *Hymenochirus* (Ueck 1967), *Spea* (DRB pers. obs.), and *Ceratophrys* (Fry and Kaltenbach 1999). In contrast to other carnivorous tadpoles, *Lepidobatrachus* tadpoles have adult-like intestinal histology (Ruibal and Thomas 1988; Ulloa Kreisel 2002) and feed

continuously without a fasting period during metamorphosis, presumably due to the lack of a need for intestinal remodeling. In *Ceratophrys*, there appears to be a reduction in histological changes to the larval stomach and intestine, including less epithelial cell apoptosis and proliferation compared to herbivorous tadpoles (Fry and Kaltenbach 1999; Kaltenbach et al. 2012). This perhaps explains the ability to continue feeding throughout metamorphosis in the face of intestinal remodeling observed in some carnivorous tadpoles (Fry and Kaltenbach 1999). The very short spiral intestine of *Hymenochirus* also does not appear to undergo metamorphic remodeling (Hintze-Podufal and Schroer 1989), but whether they feed during metamorphosis is not known. We found that the alimentary tract in *O. baluensis* has a larval stomach and intestine features similar to *Lepidobatrachus*, yet it remains unknown whether *O. baluensis* discontinues feeding during metamorphosis.

Another generalization related to diet is that obligate carnivores have large, proteolytically active stomachs relative to the smaller less enzymatically active herbivorous/omnivorous stomachs (Stevens and Hume 1995). Most tadpole species, including *Rana*, *Xenopus*, and microhylids, have a larval stomach called the manicotto glandulare (Lambertini 1929; Griffiths 1961). Bufonids and megophryids examined by Griffiths lacked a manicotto, and *Alytes obstetricans* and *Raorchestes gryllus* had highly modified manicottos. The manicotto glandulare is a uniquely larval, mucous-secreting, non-muscular section of the digestive tract between the esophagus and midgut, anterior to the gastroduodenal loop (Bloom et al. 2013). It can be found embedded with exocrine pancreatic tissue, a condition present in more basal vertebrates; yet it is not expanded for food storage in most species (Griffiths 1961). During embryonic development, the pancreas forms as an out-pocketing of the developing endoderm. It passes through a phase consisting of the forming pancreas itself, residual pancreatic tissue still present in the intestinal wall (the manicotto), and a bridge of tissue connecting the two. The manicotto is not considered a true stomach because it lacks decreased pH or pepsin activity. However, trypsin and other peptidase activity were found in some taxa, perhaps reflecting pancreatic contribution, though lipolytic or amylase activity was not found (Griffiths 1961). During metamorphosis, the manicotto epithelium degenerates and is replaced by proliferative epithelium giving rise to at least some if not all of the adult stomach (Ishizuya-Oka and Shimozawa 1987; Griffiths 1961). The tryptic activity of the manicotto does not overlap in time with the peptic activity of the definitive stomach during metamorphosis (Griffiths 1961). The midgut region of carnivorous tadpoles diverges from this description of the manicotto. Carnivorous tadpoles have an enlarged foregut storage chamber

which may have pepsin activity, i.e., *Lepidobatrachus* (Carroll et al. 1991) or not, i.e., *Hymenochirus* (Ueck 1967). The peptic activity of the enlarged foregut of *Ceratophrys* is not known (Griffiths 1961). Evolution of the heterochronic stomach with pepsin expression in *Lepidobatrachus* appears to be due to a shift in timing of retinoic acid signaling during embryonic development (Bloom et al. 2013). Consistent with previous observations in other species of the genus, we found that *O. baluensis* has a greatly expanded foregut storage chamber (Figs. 3, 8; Griffiths 1961), but the enzymatic activity is not known. In addition, in both *Occidozyga* and *Lepidobatrachus,* the larval foregut (larval stomach) is muscularized in contrast to the manicotto glandulare in herbivorous/omnivorous larvae (Griffiths 1961).

Phylogenetic interpretation of morphological features

The anatomical three-dimensional analysis recovered a remarkable number of features that are unusual for acosmanuran tadpoles (Type IV-tadpoles sensu Orton 1953, excluding microhylids) and even tadpoles in general (Sokol 1981; Haas 2003; Roček 2003). Recent phylogenetic analysis put *Occidozyga* into the subfamily Occidozyginae (apomorphy: lack of keratodonts) at the base of and sister taxon to all other members of the family Dicroglossidae, as part of the large ranoid assemblage (Frost et al. 2006; Pyron and Wiens 2011; Zhang et al. 2013). Within the Dicroglossidae, larval character states have been published for *Quasipaa exilispinosa* (described as *Paa exilispinosa*) and *Limnonectes leporinus* (Haas 2003). The same study contains data of the more distantly related *Pyxicephalus adspersus* (Pyxicephalidae), *Tomopterna cryptotis* (Pyxicephalidae), *Rana temporaria* (Ranidae), *Hylarana nigrovittata* (Ranidae), and *Ptychadena mascareniensis* (Ptychadenidae) that allow for a preliminary phylogenetic interpretation of character states. In Fig. 9, we arranged these species according to the extensive phylogeny of amphibians (Pyron and Wiens 2011), yet in condensed from, omitting all taxa in between for which no detailed cranial musculoskeletal data of the larva are available. A recent alternative phylogeny (Zhang et al. 2013) disagrees on the placement of Ptychadenidae, but these differences will not be crucial for the discussion of *O. baluensis* intended here. Based on this phylogenetic tree and the cranial character states in Haas (2003), a preliminary phylogenetic assessment can be given for the character states in present in *O. baluensis*.

For the following discussion, we refer to cranial characters as in Haas (2003) by numbers in brackets [*character*]. All character states for which this taxon sample shows no variation need no consideration [Haas 2003: 1–2, 6–7, 10, 16–19, 21, 27–28, 30–33, 36, 38, 41–43, 45, 47–53, 55,
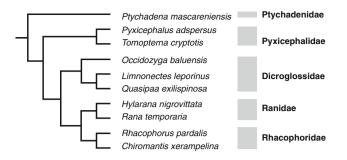
Fig. 9 Phylogenetic framework to assess character states in *Occidozyga baluensis*. Taxa that are relatively closely related to *O. baluensis* and for which morphological data of larval musculoskeletal characters are available (de Jongh 1968; Haas 1999, 2003; Sheil 1999). The phylogenetic tree was obtained by extracting phylogenetic relationships for taxa with morphological data from Pyron and Wiens (2011) and omitting all taxa without morphological information in between. Thus, *Limnonectes leporinus* and *Quasipaa exilispinosa* are the relatives closest to *O. baluensis* for which detailed larval musculoskeletal data have been published. See text for details

59–64, 69–70, 73–76, 79, 81, 84–86, 88, 90–95, 97–98, 103–104, 106–107, 109, 113, 115, 118, 120, 124, 127–133]. Given the phylogenetic position of *O. baluensis* among the taxa considered (Fig. 9), all characters in which *O. baluensis* differs from all other ranoids compared to here will be candidate autapomorphic features of *O. baluensis*, some with no equivalent character state in Haas' (2003) list and pending further testing in more comprehensive taxon samples.

Keratodont rows absent [3–5]; lip papillation absent [8–9]; eye position dorsolateral, oriented anteriorly [11]; m. interhyoideus posterior and m. diaphragmato-praecordialis absent [23–26; also in *Pyxicephalus adspersus*]; m. subarcualis rectus I portion with origin from Ceratobranchiale II absent [34]; mm. levatores arcuus branchialium relatively narrow [40]; m. suspensorioangularis with origin at postorbital level [44]; origin of the m. suspensoriohyoideus unique (pars posterior quadrati) [46]; m. levator mandibulae internus with low origin but no processus ascendens present [58]; curvatura posterior reduced (pars posterior quadrati and cartilago praeotica possible homologs of the curvatura) [68]; processus ascendens and suspensorium absent [71–72]; processus muscularis present [79–80], but in a unique conformation unknown from any other tadpole; absence of tectal cartilages, except for tectum synoticum [96]; lack of a distinct processus urobranchialis [108]; all spicula, except Spiculum II, absent [112–113]; processus anterlolateralis indistinct [116–117]; gill canal between ceratohyale and Certobranchiale I closed [123; also in *Rhacophorus pardalis*]; ligamentum cornuquadratum absent [125–126]; and branchial food traps, crescentic organs, and secretory ridges (epithelial structures for suspension feeding) absent [134–136].

Additional autapomorphies, not represented as characters in the matrix of Haas (2003), include the anterior extension of the m. abdominis system (here m. abdominis anterior) that has been reported in convergent cases elsewhere and is not fully understood (Haas and Richards 1998; Haas et al. 2006; Vera Candioti 2008). More striking is the absence of the fenestra subocularis. It has not been reported in anuran larvae (except for the leiopelmatid *Ascaphus truei* (Pusey 1943) in a different structural context). For *O. baluensis,* we conclude from the arrangement of the m. levator mandibulae internus that most likely the fenestra has been replaced secondarily by an extremely broad commissura quadrato-cranialis anterior (therefore, characters such as processus pterygoideus [77] and arcus subocularis [82] not applicable). The commissura is the only synchondrotic connection of the palatoquadrate to the neurocranium; the processus ascendens is absent in *O. baluenis*. The articulation of the palatoquadrate with the ceratohyale is posterior to the eye (at eye level or anterior to it in most other species). The derived palatoquadrate features, the sole connection of the palatoquadrate to the neurocranium (a confluence of the palatoquadrate with the capsula auditiva is absent), the special shape of the processus muscularis, the reduction in the curvatura posterior, and the loss of the processus ascendens, are to our knowledge unique character states for any tadpole examined so far. The reduction in Ceratobranchiale I is unique, although other parts of the branchial basket have been reported reduced in other species, for example, C.IV in *Atelopus* (Lavilla and de Sá 2001) or lack of commissurae terminales in *Leptobrachella mjobergi* (Haas et al. 2006).

Further studies need to corroborate whether or not these anatomical features apply to the other species of *Occidozyga* and are in fact synapomorphic features for the species contained in the genus. The genus currently contains 12 species (Frost 2013), and tadpoles are still unknown for some (Iskandar et al. 2011). Despite this lack of information, known records show some homogeneity within the genus with respect to at least some characters: *O. lima*, *O. laevis*, and *O. sumatrana* all have small, terminal, tube-like mouths as in *O. baluensis* (Alcala 1962; Heyer 1973; Inger 1985; Iskandar 1998; Leong and Chou 1999; Smith 1916). The lack of keratodont rows has been postulated as synapomorphic feature for the members of the Occidozyginae (Frost et al. 2006).

Orton (1953) defined four general free-living tadpole morphotypes, Type I–IV. In this scheme, they differ by oral structures, opercular architecture, spiracular position, but also in anatomical characters (Sokol 1975; see a recent discussion of this typological concept in Roelants et al. 2011). The four morphotypes have proven to be a handy predictor for tadpoles within the respective clade and correlate in their generality with current ideas of frog phylogeny (Sokol 1975; Cannatella

1999; Púgener et al. 2003; Roelants et al. 2011). They occupy well-separated regions in morphospace that are in accord with Triassic and Early Jurassic radiations (Roelants et al. 2011). The fact that early-diverged lineages have morphologically distinct larvae may indicate a basal period of high larval morphological innovation in the Anura partially driven by separation in ecological niches: obligate suspension feeding in Xenanura (Pipidae + Rhinophrynidae) and Microhylidae, rasping in Costata and Acosmanurans (except the Microhylidae) (Altig and Johnston 1989; Altig and McDiarmid 1999; but see Wassersug 1984, 1989; Wassersug and Pyburn 1987). The limitation of the typological concept is that Orton developed the morphotypes on a rather limited set of characters (mouthparts, spiracle), resulting in an oversimplified picture of the extant tadpole morphological and ecological diversity, and a normative (typological) restriction of the multidimensional morphological space (Wassersug 1984; Altig and Johnston 1989; Altig and McDiarmid 1999; Haas 2003; Haas et al. 2006; Roelants et al. 2011).

Occidozyga baluensis is nested deeply within the Neobatrachia that contains 96 % of all living frog species (Frost et al. 2006; Pyron and Wiens 2011; Roelants et al. 2007; Zhang et al. 2013). Cases of convergence in eco-morphological larval forms and homoplastic characters within the Neobatrachia have been long known (Altig and McDiarmid 1999; Orton 1953). The two-dimensional analysis of larval morphological data from a broad range of taxa has shown that the two-dimensional morphospace occupied by neobatrachian tadpoles was compact, lacked structural innovation, except for the derived microhylid tadpoles, and exhibited notable homoplasy (Roelants et al. 2011). In that study, the most distant outlier from the remaining neobatrachian cluster was the carnivorous larva of *Lepidobatrachus laevis*.

The list of unique features in *O. baluensis* suggests a similar outlier position of this taxon relative to the majority of neobatrachian tadpoles; viz., *O. baluensis* likely defines a new area of tadpole morphospace not yet represented in Roelants et al. (2011). In this context of morphospace and number of unique features as well as unusual ecological niche, these tadpoles are extreme among their ranid relatives. The many derived features in *Occidozyga* have evolved in 60–100 million years (Roelants et al. 2007; Zhang et al. 2013), when many other acosmanurans have had slow morphological larval evolution (Roelants et al. 2011). The understanding of the larval evolution in the Anura requires the careful investigation of the full range of anuran tadpoles, particularly "extreme" cases (Haas et al. 2006). The cranium is the structural interface of the organism for food uptake, so that significant changes in the cranial structure can be linked to derived ecological niches and feeding strategies, for which *Occidozyga* is a good example. However, there are tadpoles with significant numbers of derived features in which the feeding habits and resource partition are still unknown (Haas et al. 2006).

References

Ablan D (2008) Official Luxology modo 301 guide. Course Technology, Cengage Learning, Boston

Alcala AC (1962) Breeding behavior and early development of frogs of Negros, Philippine Islands. Copeia 1962:679–726

Altig R, Johnston GF (1989) Guilds of anuran larvae: relationships among developmental modes, morphologies, and habitats. Herpetol Monogr 3:81–109

Altig R, McDiarmid RW (1999) Diversity: familial and generic characterizations. In: McDiarmid RW, Altig R (eds) Tadpoles: the biology of anuran larvae. University of Chicago Press, Chicago, pp 295–335

Altig R, Whiles M, Taylor C (2007) What do tadpoles really eat? Assessing the trophic status of an understudied and imperiled group of consumers in freshwater habitats. Freshw Biol 52:386–395

Bloom S, Ledon-Rettig C, Infante C, Everly A, Hanken J, Nascone-Yoder N (2013) Developmental origins of a novel gut morphology in frogs. Evol Dev 15:213–223

Boulenger GA (1896) Descriptions of new batrachians in the British Museum. Ann Mag Nat Hist 6:401–406

Bragg AN (1956) Dimorphism and cannibalism in tadpoles of *Scaphiopus bombifrons* (Amphibia, Salientia). Southwest Nat 1:105–108

Bragg AN (1964) Further study of predation and cannibalism in spadefoot tadpoles. Herpetologica 20:17–24

Brower AVZ, Schawaraoch V (1996) Three steps of homology assessment. Cladistics 12:265–272

Cannatella D (1999) Architecture: cranial and axial musculoskeleton. In: McDiarmid RW, Altig R (eds) Tadpoles: the biology of anuran larvae. University of Chicago Press, Chicago

Carroll EJ, Senevirantne AM, Ruibal R (1991) Gastric pepsin in an anuran larva. Dev Growth Differ 33:499–507

Cei JM (1968) Notes on the tadpoles and the breeding ecology of *Lepidobatrachus* (Amphibia: Ceratophryidae). Herpetologica 24:141–146

Crump ML (1992) Cannibalism in amphibians. In: Elgar MA, Crespi BJ (eds) Cannibalism: ecology and evolution among diverse taxa. Oxford University Press, Oxford, pp 256–276

Das I (1995) Comparative morphology of the gastrointestinal tract in relation to diet in frogs from a locality in south India. Amphibia-Reptilia 16:289–293

De Beer GR (1937) The development of the vertebrate skull. The University of Chicago Press, Chicago

De Jongh HJ (1968) Functional morphology of the jaw apparatus of larval and metamorphosing *Rana temporaria*. Neth J Zool 18:1–103

De Jongh HJ, Gans C (1969) On the mechanism of respiration in the bullfrog, *Rana catesbeiana*. J Morphol 127:259–290

De Pinna MCC (1991) Concepts and tests of homology in the cladistic paradigm. Cladistics 7:367–394

Deban SM, Olson WM (2002) Suction feeding by a tiny predatory tadpole. Nature 420:41–42

Dietrich HF, Fontaine AR (1975) A decalcification method for ultrastructure of echinoderm tissues. Stain Technol 50:351–354

Dingerkus G, Uhler LD (1977) Enzyme clearing of Alcian Blue stained whole small vertebrates for demonstration of cartilage. Stain Technol 52:229–232

Dodd JM (1950) Ciliary feeding mechanism in anuran larvae. Nature 165:283

Drewes RC, Altig R, Howell KM (1989) Tadpoles of three frog species endemic to the forests of the Eastern Arc Mountains, Tanzania. Amphibia-Reptilia 10:435–443

Fabrezi M (2011) Heterochrony in growth and development in anurans from the Chaco of South America. Evol Biol 38:390–411

Fabrezi M, Lobo F (2009) Hyoid skeleton, its related muscles, and morphological novelties in the frog *Lepidobatrachus* (Anura, Ceratophryidae). Anat Rec 292:1700–1712

Fabrezi M, Quinzio SI (2008) Morphological evolution in Ceratophryinae frogs (Anura, Neobatrachia): the effects of heterochronic changes during larval development and metamorphosis. Zool J Linn Soc 154:752–780

Fox S (1990) Opportunistic cannibalism in tadpoles of the Great Basin Spadefoot Toad, *Scaphiopus intermontanus*. MA Thesis, San Francisco State University

Frost DR (2013) Amphibian Species of the World: an Online Reference. Version 5.6 (9 Jan 2013). Accessible at: http://research.amnh.org/herpetology/amphibia/. American Museum of Natural History, New York

Frost DR, Grant T, Faivovich J, Bain RH, Haas A, Haddad CFB, De Sá RO, Channing A, Wilkinson M, Donnellan SC, Raxworthy CJ, Campbell JA, Blotto BL, Moler P, Drewes RC, Nussbaum RA, Lynch JD, Green DM, Wheeler WC (2006) The amphibian tree of life. Bull Am Mus Nat Hist 297:1–370

Fry AE, Kaltenbach JC (1992) Gastrointestinal tract length in two species of anuran tadpoles, *Ceratophrys ornata* and *Rana pipiens*. Am Zool 32:23A

Fry AE, Kaltenbach JC (1999) Histology and lectin-binding patterns in the digestive tract of the carnivorous larvae of the anuran *Ceratophrys ornata*. J Morphol 241:19–32

Gaupp E (1893) Beitraege zur Morphologie des Schaedels. I. Primordial-Cranium und Kieferbogen von *Rana fusca*. Morphol Arb 2:275–481

Gaupp E (1894) Beitraege zur Morphologie des Schaedels. II. Das Hyo-Branchial-Skelet der Anuren und seine Umwandlung. Morphol Arb 3:389–437

Gaupp E (1896) Ecker's und Wiedersheim's Anatomie des Frosches. Erste Abteilung, Lehre vom Skelet und vom Muskelsystem. Friedrich Vieweg und Sohn, Braunschweig

Gosner KL (1960) A simplified table for staging anuran embryos and larvae with notes on identification. Herpetologica 16:183–190

Gradwell N (1972) Gill irrigation in *Rana catesbeiana*. Part I. On the anatomical basis. Can J Zool 50:481–499

Griffiths I (1961) The form and function of the foregut in anuran larvae (Amphibia: Salientia) with particular reference to the Manicotto Glandulare. Proc Zool Soc Lond 137:249–283

Grosjean S, Vences M, Dubois A (2004) Evolutionary significance of oral morphology in the carnivorous tadpoles of tiger frogs, genus *Hoplobatrachus* (Ranidae). Biol J Linn Soc 81:171–181

Haas A (1997) The larval hyobranchial apparatus of discoglossoid frogs: its structure and bearing on the systematics of the Anura (Amphibia: Anura). J Zool Syst Evol Res 53:179–197

Haas A (1999) Larval and metamorphic skeletal development in the fast developing frog *Pyxicephalus adspersus* (Anura, Ranidae). Zoomorphology 119:23–35

Haas A (2001) Mandibular arch musculature of anuran tadpoles, with comments on homologies of amphibian jaw muscles. J Morphol 247:1–33

Haas A (2003) Phylogeny of frogs as inferred from primarily larval characters (Amphibia: Anura). Cladistics 19:23–89

Haas A, Hertwig S, Das I (2006) Extreme tadpoles: the morphology of the fossorial megophryid larva, *Leptobrachella mjobergi*. Zoology 109:26–42

Haas A, Richards SJ (1998) Correlations of cranial morphology, ecology, and evolution in Australian suctorial tadpoles of the genera *Litoria* and *Nyctimystes* (Amphibia: Anura: Hylidae: Pelodryadinae). J Morphol 238:109–141

Harris RN (1999) The anuran tadpole: evolution and maintenance. In: McDiarmid RW, Altig R (eds) Tadpoles: the biology of anuran larvae. The University of Chicago Press, Chicago, IL, pp 279–294

Heyer WR (1973) Ecological interaction of frog larvae at a seasonal tropical location in Thailand. J Herpetol 7:337–361

Hintze-Podufal C, Schroer H (1989) Aspects of *Hymenochirus boettgeri* development. Fortschr Zool 35:283–286

Inger RF (1985) Tadpoles of the forested regions of Borneo. Fieldiana Zool New Ser 26:1–89

Inger RF, Stuebing RB (2005) A field guide to the frogs of Borneo. Natural History Publications (Borneo), Sdn Bhd, Kota Kinabalu

Ishizuya-Oka A, Shimozawa A (1987) Development of the connective tissue in the digestive tract of the larval and metamorphosing *Xenopus laevis*. Anat Anz Jena 164:81–93

Iskandar DT (1998) The amphibians of Java and Bali. Bogor

Iskandar DT, Arifin U, Rachmansah A (2011) A new frog (Anura, Dicroglossidae) related to *Occidozyga semipalmata* Smith, 1927, from the eastern Peninsula of Sulawesi, Indonesia. Raffles Bull Zool 59:219–228

Jungfer K-H (1996) Reproduction and parental care of the coronated treefrog, *Anotheca spinosa* (Steindachner, 1864) (Anura: Hylidae). Herpetologica 52:25–32

Kaltenbach JC, Fry AE, Colpitts KM, Faszewski EE (2012) Apoptosis in the digestive tract of herbivorous *Rana pipiens* larvae and carnivorous *Ceratophrys ornata* larvae: an immunohistochemical study. J Morphol 273:103–108

Kenny JS (1969) Feeding mechanisms in anuran larvae. J Zool Lond 157:225–246

Kleinteich T, Haas A (2006) Cranial musculature in the larva of the caecilian, *Ichthyophis kohtaoensis* (Lissamphibia: Gymnophiona). J Morphol 268:74–88

Kleinteich T, Haas A (2011) The hyal and ventral branchial muscles in caecilian and salamander larvae: homologies and evolution. J Morphol 272:598–613

Lambertini G (1929) Il manicotto glandulare di *Rana esculenta* nei suoi aspetti strutturali e nelle sue evoluzioni metamorfiche durante lo sviluppo. Ric Morfol Roma 9:71–88

Lavilla EO (1990) The tadpole of *Hyla nana* (Anura: Hylidae). J Herpetol 24:207–209

Lavilla EO, de Sá R (2001) Chondrocranium and visceral skeleton of *Atelopus tricolor* and *Atelophryniscus chrysophorus* tadpoles (Anura, Bufonidae). Amphibia-Reptilia 22:167–177

Lavilla EO, Fabrezi M (1992) Anatomia craneal de larvas de *Lepidobatrachus llanensis* y *Ceratophrys cranwelli* (Anura: Leptodactylidae). Acta Zool Lilloana 42:5–11

Leong TM, Chou LM (1999) Larval diversity and development in the Singapore Anura (Amphibia). Raffles Bull Zool 47:81–137

Malkmus R, Manthey U, Vogel G, Hoffmann P, Kosuch J (2002) Amphibians and Reptiles of Mount Kinabalu (North Borneo). A.R.G. Gantner K.G., Koeltz Scientific Books, Koenigstein

McAvoy JW, Dixon KE (1977) Cell proliferation and renewal in the small intestine epithelium of metamorphosing and adult *Xenopus laevis*. J Exp Zool 202:129–138

McDiarmid RW, Altig R (1999) Tadpoles: the biology of anuran larvae. University Chicago Press, Chicago

Metscher BD (2009) MicroCT for comparative morphology: simple staining methods allow high-contrast 3D imaging of diverse non-mineralized animal tissues. BMC Physiol 9:1–14

Mulisch M, Welsch U (2010) Romeis-Mikroskopische Technik. Spektrum Akademischer Verlag, Heidelberg

Natale GS, Alcalde L, Herrera R, Cajade R, Schaefer EF, Marangoni F, Trudeau VL (2011) Underwater acoustic communication in the macrophagic carnivorous larvae of Ceratophrys ornata (Anura: Ceratophryidae). Acta Zool 92:46–53

Orton GL (1953) The systematics of vertebrate larvae. Syst Zool 2:63–75

Patterson C (1982) Morphological characters and homology. In: Joysey KA, Friday AE (eds) Problems of phylogenetic reconstruction. Academic Press, New York

Petranka JW, Kennedy CA (1999) Pond tadpoles with generalized morphology: is it time to reconsider their functional roles in aquatic communities? Oecologia 120:621–631

Pfennig DW (1992) Polyphenism in spadefoot toad tadpoles as a locally adjusted evolutionarily stable strategy. Evolution 46:1408–1420

Pomeroy, LV (1981) Developmental polymorphism in the tadpoles of the spadefoot toad *Scaphiopus multiplicatus*. PhD dissertation. University of California, Riverside

Pope CH (1931) Notes on amphibians from Fukien, Hainan, and other parts of China. Bull Am Mus Nat Hist 61:397–610

Púgener A, Maglia AM, Trueb L (2003) Revisiting the contribution of larval characters to an analysis of phylogenetic relationships of basal anurans. Zool J Linn Soc 139:129–155

Pusey HK (1943) On the head of the liopelmid frog, *Ascaphus truei*: I. The chrondrocranium, jaws, arches, and muscles of a partly-grown larva. Q J Microsc Sci 84:105–185

Pyron AR, Wiens JJ (2011) A large-scale phylogeny of Amphibia including over 2800 species, and a revised classification of extant frogs, salamanders, and caecilians. Mol Phyl Evol 61:543–583

Richter SS (2005) Homologies in phylogenetic analyses—concept and tests. Theory Biosci 124:105–120

Rieppel O, Kearney M (2002) Similarity. Biol J Linn Soc 75:59–82

Roček Z (2003) Larval development and evolutionary origin of the anuran skull. In: Heatwole H, Davies M (eds) Amphibian biology. Surrey Beatty, Sons PTY Limited, Chipping Norton, pp 1877–1995

Roelants K, Gower DJ, Wilkinson M, Loader SP, Biju SD, Guillaume K, Moriau L, Bossuyt F (2007) Global patterns of diversification in the history of modern amphibians. PNAS 104:887–892

Roelants K, Haas A, Bossuyt F (2011) Anuran radiations and the evolution of tadpole morphospace. PNAS 108:8731–8736

Ruibal R, Thomas E (1988) The obligate carnivorous larvae of the frog, *Lepidobatrachus laevis* (Leptodactylidae). Copeia 1988:591–604

Satel SL, Wassersug RJ (1981) On the relative sizes of buccal floor depressor and elevator musculature in tadpoles. Copeia 1981:129–137

Sheil CA (1999) Osteology and skeletal development of *Pyxicephalus adspersus* (Anura: Ranidae: Raninae). J Morphol 240:49–75

Shi Y-B, Ishizuya-Oka A (1996) Biphasic intestinal development in amphibians: embryogenesis and remodeling during metamorphosis. Curr Top Dev Biol 32:205–235

Smith MA (1916) On the frogs of the genus *Oxyglossis*. J Nat Hist Soc Siam 2:172–175

Sokol OM (1962) The tadpole of *Hymenochirus boettgeri*. Copeia 1962:273–284

Sokol OM (1975) The phylogeny of anuran larvae: a new look. Copeia 1975:1–23

Sokol OM (1981) The larval chondrocranium of *Pelodytes punctatus*, with a review of tadpole chondrocrania. J Morphol 169:161–183

Stevens CE, Hume ID (1995) Comparative physiology of the vertebrate digestive system. Cambridge University Press, Cambridge

Storz BL, Travis J (2007) Temporally dissociated, trait-specific modifications underlie phenotypic polyphenism in *Spea multiplicata*, which suggests modularity. Sci World J 7:715–726

Taylor EH, Elbel RE (1958) Contribution to the herpetology of Thailand. Univ Kans Sci Bull 38:1033–1189

Taylor WR, Van Dyke GC (1985) Revised procedures for staining and clearing small fishes and other vertebrates for bone and cartilage study. Cybium 9:107–119

Ueck M (1967) Der Manicotto Glandulare ("Drüsenmagen") der Anurenlarve. Z wiss Zool 176:173–270

Ulloa Kreisel ZE (2002) Caracteriticas morfologicas del tubo digestivo en larvas carnivoras de *Lepidobatrachus llanensis* (Anura: Leptodactylidae). Acta Zool Lilloana 46:31–38

Veeranagoudar DK, Radder RS, Shanbhag BA, Saidapur SK (2009) Jumping behavior of semiterrestrial tadpoles of *Indirana beddomii* (Günth.): relative importance of tail and body size. J Herpetol 43:680–684

Vera Candioti MF (2005) Morphology and feeding in tadpoles of *Ceratophrys cranwelli* (Anura: Leptodactylidae). Acta Zool 86:1–11

Vera Candioti MF (2007) Anatomy of anuran tadpoles from lentic water bodies: systematic relevance and correlation with feeding habits. Zootaxa 1600:1–175

Vera Candioti MF (2008) Larval anatomy of Andean tadpoles of *Telmatobius* (Anura: Ceratophryidae) from northwestern Argentina. Zootaxa 1938:40–60

Vera Candioti MF, Lavilla EO, Echeverria DD (2004) Feeding mechanisms of two treefrogs, *Hyla nana* and *Scinax nasicus* (Anura: Hylidae). J Morph 261:206–224

Wassersug RJ (1980) Internal oral features of larvae from eight anuran families: functional, systematic, evolutionary, and ecological considerations. Misc Pub Mus Nat Hist Kans 68:1–146

Wassersug R (1984) The *Pseudohemisus* tadpole: a morphological link between microhylid (Orton type 2) and ranoid (Orton type 4) larvae. Herpetologica 40:138–149

Wassersug RJ (1989) What, if anything is a microhylid (Orton type II) tadpole? In: Splechtna H (ed) Trends in vertebrate morphology. G. Fischer, Stuttgart, pp 534–538

Wassersug R, Heyer WR (1988) A survey of internal oral features of leptodactylid larvae. Smith Contr Zool 457:1–99

Wassersug RJ, Pyburn WF (1987) The biology of the Pe-ret' toad *Otophryne robusta* (Microhylidae), with special consideration of

its fossorial larva and systematic relationships. Zool J Linn Soc 91:137–169

Zhang P, Liang D, Mao RL, Hillis DM, Wake DB, Cannatella DC (2013) Efficient sequencing of anuran mtDNAs and a mitogenomic exploration of the phylogeny and evolution of frogs. Mol Biol Evol 30:1899–1915

Ziermann JM, Infante C, Hanken J, Olsson L (2011) Morphology of the cranial skeleton and musculature in the obligate carnivorous tadpole of *Lepidobatrachus laevis* (Anura: Ceratophryidae). Acta Zool 94:101–112